

LA-UR-18-21291 (Accepted Manuscript)

Impact Sensitivity and Ignition Mechanisms of Nanoaluminum-poly(perfluorinated methacrylate) Nanocomposites

Morris, Lauren A.
Thompson, Darla Graff
DeLuca, Racci
Shelbourne, Ian
Gunduz, Emre
Son, Steve
Haines, Chris

Provided by the author(s) and the Los Alamos National Laboratory (2018-11-14).

To be published in: MRS Advances

DOI to publisher's version: 10.1557/adv.2018.339

Permalink to record: <http://permalink.lanl.gov/object/view?what=info:lanl-repo/lareport/LA-UR-18-21291>

Disclaimer:

Approved for public release. Los Alamos National Laboratory, an affirmative action/equal opportunity employer, is operated by the Los Alamos National Security, LLC for the National Nuclear Security Administration of the U.S. Department of Energy under contract DE-AC52-06NA25396. Los Alamos National Laboratory strongly supports academic freedom and a researcher's right to publish; as an institution, however, the Laboratory does not endorse the viewpoint of a publication or guarantee its technical correctness.

Impact Sensitivity and Ignition Mechanisms of Nanoaluminum-poly(perfluorinated methacrylate) Nanocomposites

Lauren A. Morris,^{*,†} Darla Graff Thompson,[†] Racci DeLuca,[†] Ian Shelburne,[§] I. Emre Gunduz[‡], Steven F. Son,[‡] and, Chris D. Haines[†]

[†]Armament Research, Development and Engineering Center, U.S. Army RDECOM-ARDEC, Picatinny Arsenal, New Jersey 07806

[†]M-7, HE Mechanical Testing Los Alamos National Laboratory, Los Alamos, New Mexico 87545

[§]School of Aeronautics and Astronautics, Purdue University, West Lafayette, Indiana 47904

[‡]School of Mechanical Engineering, Purdue University, West Lafayette, Indiana 47907

*corresponding author e-mail: lauren.a.morris17.civ@mail.mil

ABSTRACT

Nanoenergetic composites are of overwhelming interest to the Department of Defense because of the high power output and the ability to finely tune the ignition thresholds of these composites. Recently, several variants of a nanoaluminum-poly(perfluorinated methacrylate) (AlFA) have been synthesized and optimized for a variety of applications including reactive warhead liners and bullet spotters. While conventional techniques such as thermal analysis and bomb calorimetry can be used to characterize the reaction mechanism and energy output of AlFA composites, characterizing their dynamic behaviour is more challenging. Bullet spotter applications require a material to be impact sensitive at very low velocities, yet be adequately **insensitive**. Several live-fire tests were conducted which revealed the AlFA₅₀ material reacted consistently upon target impact at high velocities, but unreliably at very low velocities. In an effort to better understand the fundamental impact ignition mechanism and to determine the impact velocity threshold of AlFA₅₀ a series of Taylor gas gun experiments were conducted. It was determined that the light-initiation mechanism was consistent with a pinch mechanism, and that the ignition velocity threshold was near 74 m/s. Based on these results, it was hypothesized that the addition of a filler material could be used to sensitize the AlFA₅₀, and that Asay shear impact testing could be used to determine a more optimal shape of such inclusions. Experiments performed using the Asay shear impact test setup confirmed the pinch ignition mechanism, but observations also revealed that the size of the pinch point was important. Finally, it was shown that the addition of large glass beads (> 1mm in diameter) was effective at sensitizing the AlFA₅₀ material at high and low velocities, with ignition observed at impact velocities as low as 35 m/s.

I. INTRODUCTION

Reactive nanocomposites are an exciting new class of materials whose properties can be tuned for a variety of special effects. Although the need exists, the US Army does not have any safe ammunition that allows gunners in training exercises to easily observe projectile impact events on target. Current ammunition does not provide an impact signature and/or marking capability to produce visible (day and night) and/or infrared (IR) signatures at distances by simple means. In the past, most proposed solutions to this issue have included using explosives, pyrotechnics, or chemical “cocktails” to achieve this desired effect; unfortunately, this often results in duds and un-explored ordinance (UXO) on the battlefield and/or training facility, posing unnecessary safety issues for the Soldiers and firing range staff. Another proposed solution included using pyrophoric powders, but after-burn effects pose fire hazards on the training ranges. Furthermore, training projectiles are not typically hermetically sealed, causing the pyrophoric materials to prematurely oxidize and lose their effectiveness. As a result, ARDEC began investigating the use of an air-stable reactive nanocomposite as a novel payload for a new class of non-UXO visible/thermal spotter munitions. The requirements were that the payload material be applicable for a number of munition systems and demonstrate impact sensitivity over a range of velocities (50-1000 m/s) and from a range of distances (100-1000 m from target).

The synthesis and reactivity of a variety of nanoaluminum-poly(perfluorinated methacrylate) (AIFA) nanocomposites has been reported extensively by Crouse et al. [1-4]. Essentially, the AIFA nanocomposite consists of 80 nm nanoaluminum (nAl) embedded in a fluorinated polymeric acrylate matrix, synthesized via in situ polymerization on the surface of oxide passivated nAl. The nanocomposite AIFA has demonstrated high exothermic reactivity with variable nAl particle loading up to 60 % by weight [1]. Furthermore, it was demonstrated that AIFA reacts on impact at velocities greater than 100 m/s in air and in a vacuum [2]. Crouse et al. have reported that the reaction mechanism of the AIFA composite is a combination of aluminium fluorination, oxidation, and carburization, and that its reaction pathway and kinetics are dependent on the solids loading (i.e. amount of nAl) and amount of oxygen available during reaction [1]. Recently, White et al. used modified Taylor impact testing and modelling to conclude that the reaction of AIFA with 50 wt.% nAl, or AIFA₅₀, was mechanically initiated in the shear bands generated by compaction of AIFA₅₀ at the anvil [5].

Due to its impact sensitivity and tunable properties, it was determined that AIFA should be considered a candidate material for spotter munitions. Additionally, it is air-stable and can be processed easily by a variety of techniques due to its thermoplastic behavior. A series of experiments were executed to characterize the performance of AIFA as a bullet spotter material, as well as to confirm and to better understand the mechanically induced ignition mechanism at work in the nanocomposite. Live-fire ballistic testing was used to determine if the AIFA nanocomposite’s reaction signature met the requirements, and to determine if it could be initiated over the entire velocity range. When the AIFA₅₀ nanocomposites struggled to react consistently at low velocities (< 100 m/s) subsequent Taylor impact tests were performed to confirm the ignition mechanism upon impact. Furthermore, it was hypothesized that the velocity threshold of ignition in AIFA could be reduced by the inclusion of a filler material that may create additional shear bands within the composite. To test this hypothesis, Asay shear impact testing was conducted on neat AIFA as well as AIFA loaded with filler materials. Thermochemical modelling software was also employed as a way to explore the available reaction chemistries under equilibrium conditions.

II. EXPERIMENTAL DESIGN

All of the AIFA specimens prepared for this effort were nanoaluminum-poly(perfluorinated methacrylate) with 50 wt.% nanoaluminum (80 nm, oxide passivated), herein designated as AIFA₅₀. The AIFA₅₀ was synthesized via in situ polymerization according to chemistry described by Crouse et al. [1,3]. The weight percent of nAl in the synthesized nanocomposite was confirmed by thermogravimetric analysis to be 50 ± 3 % by weight. In all cases the neat AIFA₅₀ powder was homogenized in a DACA twin-screw extruder at 250 RPM and 165 °C for 5 minutes and the extrudate was allowed to cool to room temperature before being ground into a powder using a mortar and pestle. The specimens used for testing were either prepared by hot-pressing or hand-molding. For the hot-pressed samples AIFA₅₀ powder was loaded into a mold of the required size and shape and heated to 180 °C under 1000 lb pressure to produce smooth, uniform samples. For the hand-molded samples AIFA₅₀ powder was heated using an oil bath or hot plate at 180 °C. Knowing the density of the AIFA₅₀ (2.14 g/cc) the appropriate mass of AIFA₅₀ powder was placed in a beaker if using an oil bath or on a steel plate if using a hot plate and allowed to melt. The warm AIFA₅₀ was then molded into the required geometry using a spatula, folded into itself to thoroughly remove excess air bubbles and voids from the final sample, and then allowed to cool to room temperature. Once cooled, the sample was removed from the mold. For the tests that required the addition of a filler material, all AIFA₅₀ sample preparations followed these hand-molding procedures only differentiating the amount of AIFA₅₀ and filler material on a volume basis.

a. Ballistic testing

Ballistic testing was conducted at the US Army’s Armaments Research Development and Engineering Center’s (ARDEC) Armaments Testing Facility (ATF) at Picatinny Arsenal, NJ. A schematic of the ballistic test setup is shown in Figure 1a. Both hand-pressed and hot-pressed samples (Figures 1b and 1c, respectively) were tested. In all tests specimens of AIFA₅₀ (7g) were loaded into the empty plastic ogive (nose cone) of the spotter munition and held in place with a thin layer of epoxy. In some test specimens 10 g of tungsten shot (2 mm diameter) was loaded behind the AIFA₅₀ and the remaining volume of the cavity was loaded with cotton balls to prevent shifting of the contents. The munition was then loaded into the projectile fired from a gun at velocities ranging from 50 – 1000 m/s. The ballistic testing was recorded using high-speed video.

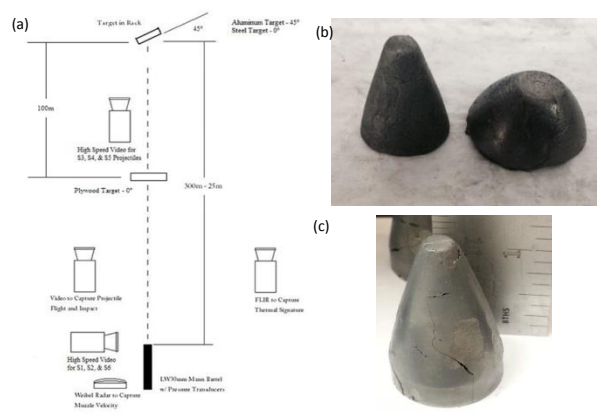


Figure 1: (a) Schematic of ballistic testing set up, (b) image of AIFA₅₀ specimens for ballistic testing as prepared by hand-molding and (c) image of AIFA₅₀ specimens for ballistic testing as prepared by hot-pressing.

b. Gas gun testing

Gas-gun testing was conducted at Los Alamos National Laboratory, NM on a 500 psi intermediate-rate gas gun (also known as a Taylor gun). As shown in Figure 2a, barrel-mounted lasers were used to trigger two flash lamps and two high-speed cameras (Phantom with top view, Photron with side view), providing ~20 microsecond frames of the specimen as it impacted a steel anvil inside a boom box. The relationship between gun pressure, sample mass, and velocity is shown in Equation 1, where A and B are predetermined constants unique to the gas gun used for this study.

$$velocity = A * \left(\frac{pressure}{mass} \right)^B \quad (1)$$

The projectiles were designed to include two different lengths of aluminum pusher (Figure 2b), allowing access to two different velocity ranges. The gun pressure was varied for each pusher type, to access a range of velocities for each. The barrel velocity was measured at the time of the test and was obtained from the sequential blocking of two lasers mounted 50.15 mm apart from each other in the barrel. The image velocity was determined from the high-speed images of the Photron camera, side-view. In the AIFA tests image velocities (after sabots are stripped) are slightly lower than barrel velocities (when the projectile and sabot are still a unit).

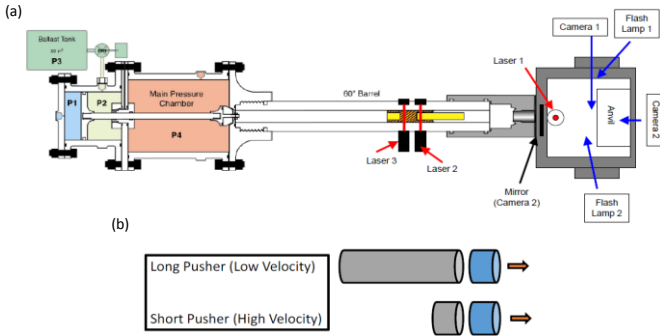


Figure 2: (a) Schematic of gas gun testing and (b) schematic of gas gun projectiles using aluminium pushers (gray) and samples of AIFA₅₀ as prepared by hot-pressing (blue).

c. Asay shear impact testing

Asay shear impact testing was conducted at Purdue University (West Lafayette, IN) to further investigate the ignition mechanism and sensitivity in AIFA₅₀. In this test, shown in Figure 3, a thin rectangular sample was supported in a windowed holder, allowing for direct imaging of the side surface of the sample. A movable plunger was also held in the sample holder and placed against the front face of the sample. This plunger was impacted at a specific velocity by a projectile that was propelled from a light gas gun. The plunger then impinges the test sample and imparts both compressive and shear strains to it. The amount of shear and compression can be tailored by modifying the geometry of the plunger's impacting

face. The strain profile can be modified from pure compression to almost pure shear. The impact was monitored using a high speed camera (Vision Research Phantom v7.3).

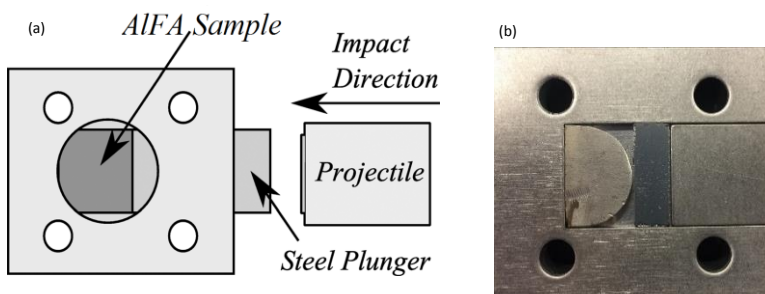


Figure 3: (a) Schematic of Asay shear impact test set-up with rectangular plunger and (b) image of Asay shear impact testing with modified parabolic plunger design loaded with an AIFA₅₀ sample.

d. Characterization and modelling

The physical and energetic properties of AIFA₅₀ in various stages of processing (neat powder, hot-pressed extrudate, hot-pressed extrudate ground powder, and hand-molded ground powder) were determined by a variety of techniques. Nitrogen adsorption isotherms were measured at 77 K using a Quantachrome Nova 4000e analyzer, and the volume of adsorbed nitrogen was normalized to standard temperature and pressure for calculation. Both adsorption and desorption isotherms were recorded, and the specific surface area was determined from the linear part of the BET equation ($P/P_0 = 0.05-0.31$). The calculation of total pore volume of AIFA materials was based on the nitrogen adsorption volume at around $P/P_0 = 0.995$. All the samples were degassed at 110 °C for at least 1 h prior to the experiments. Samples were imaged with a Keyence VHX-600 digital optical microscope. Combustion energy output of AIFA materials was measured with a Parr 618 Calorimeter with argon as purge gas and the insulating jacket temperature set at constant 35 °C. A Parr 1104 High Strength bomb with 240 ml headspace was used for concealed combustion. In a typical measurement, a measured AIFA sample of about 1.0 g was loaded into the bomb with a 10 mm Ni-alloy fuze wire for ignition. The sealed bomb with sample was then purged and pressurized with argon to 450 psig, and finally transferred to the calorimeter for testing. The total exothermic output was recorded.

Thermodynamic equilibrium calculations were performed with FactSage 7.1 (Thermfact/CRCT and GTT-Technologies). The particular databases used were FactPS, FToxid, and FTOxCN from which the reactants CF₂, Al, and O₂ were selected. Simulations were conducted at a constant pressure of 1 atm with the reactants initially at 298 K. Analyses were also performed in adiabatic mode ($\Delta H = 0$). The results consist of predicted adiabatic reaction temperatures (T_{ad}) and the thermodynamic products under those conditions.

III. RESULTS

a. Ballistic testing

The objective was to test AIFA in live-fire scenarios to determine whether the material could be initiated over a wide range of velocities (50-1000 m/s) to produce a signature applicable for bullet spotters. Very preliminary ballistic testing included specimens with 30 wt.% and 60 wt.% solids loading (AIFA₃₀ and AIFA₆₀) in addition to the 50 wt.% AIFA₅₀; however, it was determined that neither AIFA₃₀ or AIFA₆₀ were good candidates for spotter technologies due to lack of reaction upon impact, even at high velocities. Two series of ballistic tests were undertaken for AIFA₅₀; the first preliminary series used hand-molded specimens (Figure 2b) while the second series of tests used hot-pressed specimens (Figure 2c). The tests using hand-molded specimens of AIFA₅₀ epoxied into the nose cone were the first to be conducted for bullet spotter applications, and a limited number of samples were tested at high (500-300 m/s) and low (70 – 200 m/s) velocities. The hand-molded nanocomposite was observed to react somewhat inconsistently over all velocities tested; however, the composite did react successfully in 67% of high velocity tests, and in 10% of the low velocity tests. While the reliability over all velocities was low, it was determined that when the nanocomposite did react successfully, the signature was ideal for spotter munitions producing a fast, hot, bright signature at target impact with no after-burning effects. Figure 4 shows still-frame images of a successful ignition of AIFA₅₀ specimen back-loaded with tungsten shot fired at 347 m/s. A bright white light is produced upon target impact, generating a fast, hot flash indicative of the reaction of AIFA₅₀. Furthermore, the tests on the hand-molded composites demonstrated that ignition was at least possible over the entire velocity range of interest (50 – 1000 m/s).

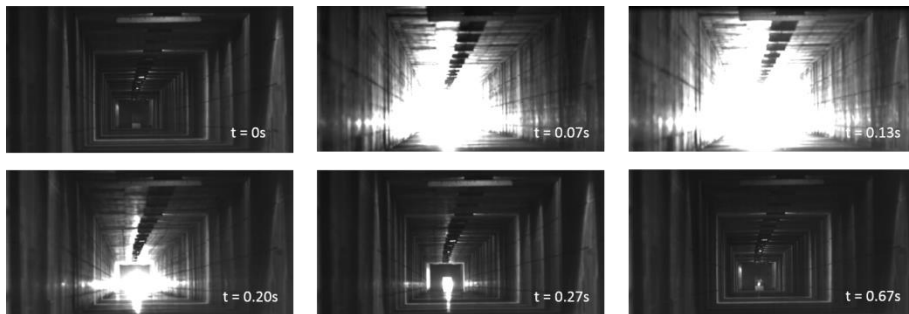


Figure 4: Still-frame images from ballistic testing of a successful ignition and reaction of AIFA₅₀ upon target impact at 347 m/s. Frames start in the upper left corner, frame numbers increase left to right, then jump to lower left corner and again move left to right.

Based on these initial promising results, a much larger ballistic test was designed. To satisfy the schedule and number of specimens required, this time AIFA₅₀ test specimens were prepared by hot-pressing as described in Section II. The AIFA₅₀ specimens were epoxied into the nose cone and fired at velocities from 70 – 350 m/s. None (0 %) of the hot-pressed AIFA₅₀ specimens reacted at any velocity, indicating that the hot-pressed specimens were much less sensitive to ignition at impact than the hand-molded specimens. In an effort to sensitize mechanically induced ignition, the rest of the ballistic test specimens of AIFA₅₀ included 10 g of tungsten shot loaded into the nose cone behind the nanocomposite. The addition of tungsten shot was successful in sensitizing the hot-pressed AIFA₅₀ for reaction over the entire velocity range. Nearly 100 specimens of hot-pressed AIFA₅₀ loaded with tungsten shot were tested at velocities ranging from 70-1000 m/s. It was observed that the ignition threshold for AIFA₅₀ in this configuration was near 80 m/s with no successful ignitions observed at velocities below 79 m/s. Table 1 summarizes the results of this testing.

Table 1: Summary of results from ballistic testing of hot-pressed AlFA₅₀ with tungsten shot over a range of impact velocities.

	v < 100 m/s	100 < v < 350 m/s	350 < v < 700 m/s	700 > v > 1000 m/s
Percent (%) successful reaction upon target impact	8	51	68	80

The results of both series of the ballistic testing indicate that there is a difference in ignition sensitivity of the hand-pressed specimens as compared to the hot-pressed specimens, and that the addition of tungsten shot was successful in sensitizing the hot-pressed samples for mechanically-induced ignition. While all samples demonstrated inconsistencies in reliability especially at low velocities, the signature that was produced, when successful, was ripe for spotter technologies.

b. Gas gun testing

A series of gas gun experiments was conducted to better understand the ignition mechanism and threshold velocity. The goal of the test was to vary the impact velocity of AlFA₅₀ projectiles in a controlled way to determine the threshold velocity for light initiation, while observing the ignition event upon impact with the anvil from both top and side perspectives.

A total of 13 shots were fired during the Taylor gun testing and for each shot it was determined if any light was produced, and if so if the light initiation was generated upon impact with the target or upon a pinch of AlFA₅₀ between the pusher and the target. Table 2 summarizes the results of the gas gun testing, including the barrel and image velocities, whether the pusher and AlFA₅₀ were intact at impact, and observations regarding whether the light initiation was observed at impact or during the pinch/confinement.

Table 2: Summary of results from gas-gun testing of AlFA₅₀ over a range of impact velocities.

Barrel Velocity (m/s)	Image Velocity (m/s)	Projectile Intact?	Light Initiation?	Impact/Pinch
AlFA ₅₀ + Short Sabot (High Velocity)				
193	182	No	Yes	Pinch
152	155.8	No	No	n/a
139	128.8	No	No	n/a
119	114.3	No	No	n/a
114	101	No	No	n/a
105	100.5	Yes	Yes	Impact
AlFA ₅₀ + Long Sabot (Low Velocity)				
70	64.5	Yes	No	n/a
73	69.2	Yes	No	n/a
73	71.4	Yes	Yes	Pinch*
75	74.2	Yes	Yes**	Pinch
77	67.5	No	Yes	Pinch

78	73.8	No	Yes	Pinch
80	77.1	No	Yes	Pinch

* extremely violent, anomalous reaction observed

** only a very small amount of light was observed

All impacts occurred with a great deal of fragmentation and powder production. When impacts did not produce light, there was almost always a hard deposit of AIFA₅₀ that remained on the anvil at the impact location. For all but one test, any observed light initiation took place during the pinch process between the anvil and the pusher. An example of a typical ignition at the pinch is shown in Figure 5a (193 m/s). Only in a single test (105 m/s) did the specimen emit light at the first moment of impact with the anvil; this test was unique in that it was the only test of the series where the anvil was not cleaned off from the prior test, and likely the anvil was rough and abrasive with hardened debris from the previous shot. See Figure 5b.

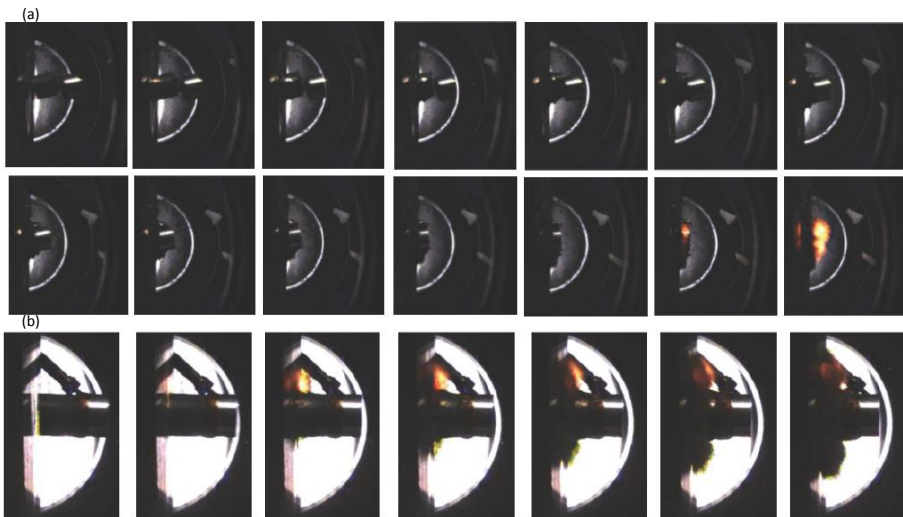


Figure 5: Sequential still-frames (12.5 μ s) from gas-gun testing of AIFA₅₀ from the Photron camera showing impact side-view. Anvil is on the left, specimen is moving right to left. Frames start in the upper left corner, frame numbers increase left to right, then jump to lower left corner and again move left to right. (a) The AIFA specimen contacts the anvil at 193 m/s in the second frame, and light is initiated 11 frames later when the specimen is pinched between the pusher and anvil. (b) The AIFA specimen contacts the anvil at 105 m/s in the second frame and light is initiated immediately or in the following frame. Note that in the subsequent frames that the light reaction appears constrained to the top half of the specimen, and the bottom half fragments and produces a great deal of powder/debris that is not consumed.

It should be noted that adhesion of the aluminium pusher to the AIFA specimen was quite problematic (especially velocities > 100 m/s), and in many tests the pusher and specimen separated before impact with the anvil, as noted in Table 2. The test plan required the AIFA₅₀ specimen to be glued to the aluminum pusher prior to testing. Superglue (cyanoacrylate), Barco Bond, and Loctite Plastics Bonded System were tried but none of these materials provided a strong enough bond to survive the launch when using a single thin layer at the specimen-pusher interface. While better adhesion was observed by reinforcing the bond joint (i.e. the adhesive ring) with two wraps of 2 mm thick Teflon tape prior to loading the part into

the sabot the solution added some lateral confinement to the impacting system; this could be considered a concern, although the data seem very consistent. As seen in Table 2, in many cases when the projectile was not intact upon target impact, no light initiation was observed further indicating a mechanically induced pinch as the ignition mechanism at play in the AlFA nanocomposite.

By stepping down the velocity of the gas gun shots the ignition threshold of AlFA₅₀ was determined to be around 75 m/s. Reactions were observed at 77 and 78 m/s, initiated at the pinch point. A small amount of light and partial reaction was observed at 75 m/s, while no light initiation was observed in one test at 73 m/s. These results are consistent with the predicted ignition threshold near 80 m/s as deduced from ballistic testing. Quite interestingly, while one of the shots fired at 73 m/s did not react, a second shot fired at 73 m/s reacted anomalously, producing an *extremely* violent reaction that was unlike any of the other observed reactions. Figure 6 compares the reaction observed at 75 m/s (6a and 6b) to the extremely violent reaction observed at 73 m/s (6c and 6d). It was immediately evident from the remote viewing location that this anomalous reaction at 73 m/s was one of the most violent ever observed on this gun, blowing the barrel away from the boom box several feet and producing a great deal of smoke. The anomalous reaction charred the barrel, adaptor, anvil, boom box and lasers, and took a week of clean-up to recover equipment to working order. Note that light initiation is more prompt on the faster test, but combustion is more complete on the slower test. From the full high-speed video of the tests, the total light duration of the test at 75 m/s was determined to be approximately 125 μ s, while the total light duration of the anomalous test at 73 m/s was determined to be approximately 18,750 μ s, much longer than any other AlFA₅₀ signature observed to date.

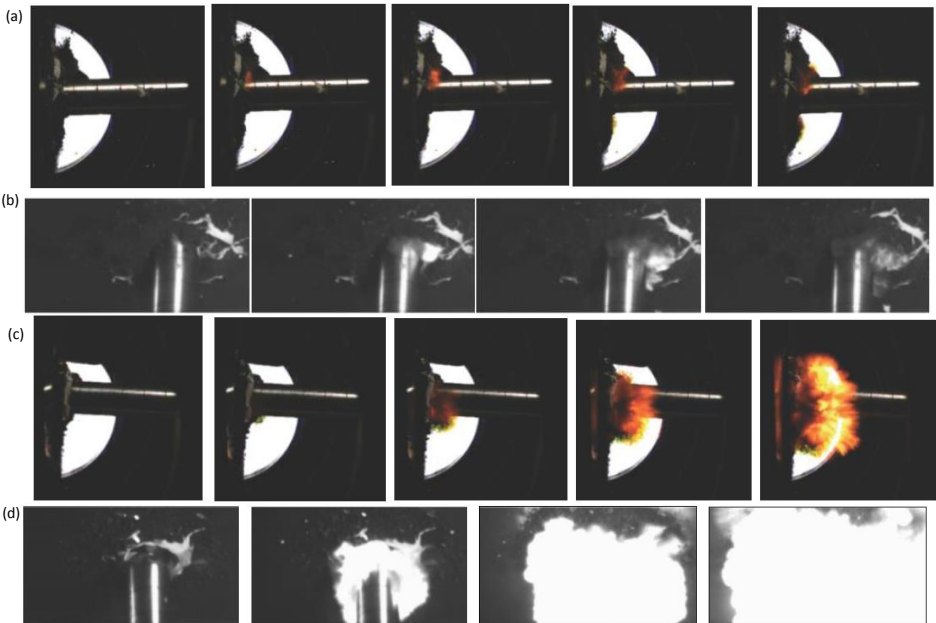


Figure 6: (a) Sequential still-frames (12.5 μ s) from the Photron camera showing impact side-view of AlFA₅₀ impact at 75 m/s. Anvil is on the left, specimen is moving right to left. Frames start on the left, frame numbers increase left to right. (b) Sequential still-frames (25 μ s) from the Phantom camera showing impact top-view of AlFA₅₀ impact at 75 m/s. Anvil is at the top, specimen is moving bottom to top. Frames start on the left, frame numbers increase left to right. (c) Sequential still-frames (12.5 μ s) from the Photron camera showing impact side-view of AlFA₅₀ impact at 73 m/s. Anvil is on the left, specimen is moving right to left. Frames start on the left, frame numbers increase left to right. (d) Sequential still-frames (25 μ s) from the Phantom camera showing impact top-view of AlFA₅₀ impact at 73 m/s. Anvil is at the top, specimen is moving bottom to top. Frames start on the left, frame numbers increase left to right.

There are two possible explanations for the extremely violent reaction observed at 73 m/s. The first possibility is that unreacted AIFA debris from previous tests was ignited by the reaction event in this shot and contributed to the increased light duration observed for this shot. Debris generated by brittle fragmentation from five previous tests was still in the boom box at the time of this shot, so any unreacted AIFA dust could have been propagated by the reacting material ignited in this shot. While this explanation is plausible, it should be noted that the propagation of reaction and light generation was more intense in the violent reaction at 73 m/s even in the first few frames of reaction (see Figure 6) before the unreacted dust would have been initiated – meaning that the violence of this reaction was stronger right out of the gate.

The second possible explanation is that the dynamics of the 73 m/s impact were just right to get a more violent than expected response. It has been suggested in literature by Perry, et al. that for a mechanically induced ignition, there may be a “sweet-spot” near the threshold ignition velocity where one might observe a more violent reaction [6-7] due to the unique dynamic confinement near the threshold velocity. The researchers from LANL discuss mechanical confinement (MC) strength as the failure strength of the structure confining an explosive when subjected to the reaction pressure, and inertial confinement (IC) as a function of the structural fragmentation dynamics of the explosive and the gas production dynamics [6]. The total reaction response can be quantified in terms of the total enthalpy change, the reactive powder, and a quantifiable measure of violence of the reaction [7]. Perry et al. express the violence (V) of a reaction (Equation 2) as a function of both the total energy released (ϵ_E) and the reactive power (ϵ_P) relative to the energy and power of detonating TNT [6].

$$V = \epsilon_P * \epsilon_E \quad (2)$$

The relationship implies that there is not only an energy dependence, but also an impulse dependence that influences the violence of an observed reaction. In one study relevant to the discussion here, Price and Wehner observe a deflagration to detonation transition (DDT) that was dependent on the IC of the fragmenting walls [8]. Other researchers have demonstrated a transition to violent reaction from nonviolent laminar burning near the ignition threshold in plastically bonded explosives (PBX) in a pressure vessel [9-10]. With these studies in mind, it is easy to imagine that if the impact velocity is fast enough to cause ignition and brittle fracture, but not fast enough to throw these unreacted fragments out of the vicinity of the propagating burn, that this unique combination of dynamic confinement might result in a more violent reaction than observed at higher velocities where the fragments might be ejected far from the reaction zone. It is more likely that this was the mechanism at play in this anomalous reaction, observed near the ignition threshold at 73 m/s given that the reaction was more violent even before propagating to unreacted AIFA dust. For the extremely violent reaction of AIFA₅₀, the closed boom box likely contributed MC unlike the previous tests, while the stochastic nature of brittle fragmentation near the threshold velocity contributed IC, thereby generating an especially violent reaction at this “sweet-spot”, as observed previously in PBX.

c. Asay shear impact testing

Asay shear impact testing was undertaken to observe ignition by the mechanically induced pinch mechanism up close, and to try to sensitize AIFA₅₀ for reliable ignition at velocities less than 100 m/s. Three tests were initially performed on hot-pressed AIFA₅₀ using the test set-up shown in Figure 3a with a rectangular plunger design. In two tests conducted with a plunger velocity of 121 m/s ignition was observed along the back wall/corner of the test section. The observed ignition delays of AIFA₅₀ at 190 m/s were 176 and 242 μ s. In a test conducted at 81 m/s the AIFA₅₀ failed to react using the rectangular plunger. These initial baseline experiments further confirmed the pinch mechanism responsible for ignition. It was hypothesized that AIFA₅₀ could be sensitized for ignition by inducing a large pinch in the material. To test this hypothesis, a modified parabolic plunger (Figure 3b) was designed to induce more shear forces on the test specimen. With the modified design, successful ignition of AIFA₅₀ was observed at the pinch point at 127 and 91 m/s (see Figure 7).

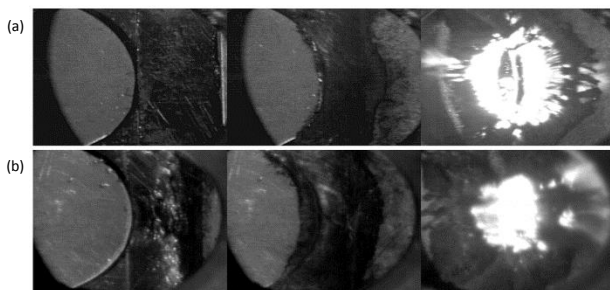


Figure 7: Still-frame images from Asay shear impact testing of AIFA₅₀ using the modified parabolic plunger design showing ignition at the pinch point at (a) 127 m/s and (b) 91 m/s.

It has been reported in literature that the inclusion of grit and other filler materials in a mechanically initiated PBX can cause increased temperatures in shear bands around the grit which are formed at target impact [11]. These increases in temperatures cause localized hot-spots within the material that induce ignition at impact thresholds lower than those observed in the neat material. Asay shear impact testing was used to test the hypothesis that a filler material could be added to AIFA to further sensitize ignition at low velocities. Microballoons were selected as the first inclusion material. Nanocomposite specimens were prepared with 10, 15, and 35 volume percent microballoons and the specimens were tested in the Asay shear impact tester with parabolic plunger design. Although initial results were promising, showing decreased time to ignition for samples containing 10 vol.% microballoons, additional testing revealed that these results were not consistent and repeatable.

The second filler material, glass beads (> 1 mm in diameter), was selected for its larger size, with the hope that larger inclusions would generate larger pinch points, more indicative of those created with the parabolic plunger. The results of tests performed on samples containing 15 vol.% glass beads are summarized in Table 3.

Table 3: Summary of results from Asay shear impact testing using the parabolic plunger design of AIFA₅₀ with the addition of large glass beads as a filler material.

AIFA ₅₀ (vol.%)	Filler Material	Plunger Velocity (m/s)	Ignition Delay (μs)
85	Glass Beads	124	69
85	Glass Beads	115	73
85	Glass Beads	105	90
85	Glass Beads	69	120
85	Glass Beads	52.2	273
85	Glass Beads	35.1	378

Results from these extremely low velocity tests showed a clear reduction in the time to ignition, initiation of reaction along the face of the plunger, and in general a reaction at low plunger velocities not previously seen. With the addition of 15 vol.% glass beads, ignition was observed at a plunger velocity of 35 m/s, less than half of the previously determined ignition threshold velocity for unfilled AIFA₅₀. In addition to drastically lowering the ignition threshold, the inclusion of glass beads also reduced the ignition delay time, especially at higher velocities. For the specimens that contained 85 vol.% AIFA₅₀ and 15 vol.% glass beads, the ignition delay time (μs) versus plunger velocity (m/s) curve fits well with the power law curve shown in Equation 3 for velocities from 35-125 m/s.

$$\text{ignition delay time} = 56078(\text{impact velocity})^{-1.370} \quad (3)$$

The exponent in this equation is cut off.

Figure 8 shows still frame images collected by high-speed video of 85 vol.% AIFA₅₀ and 15 vol.% glass beads including ignition at the lowest velocity observed to date, 35 m/s.

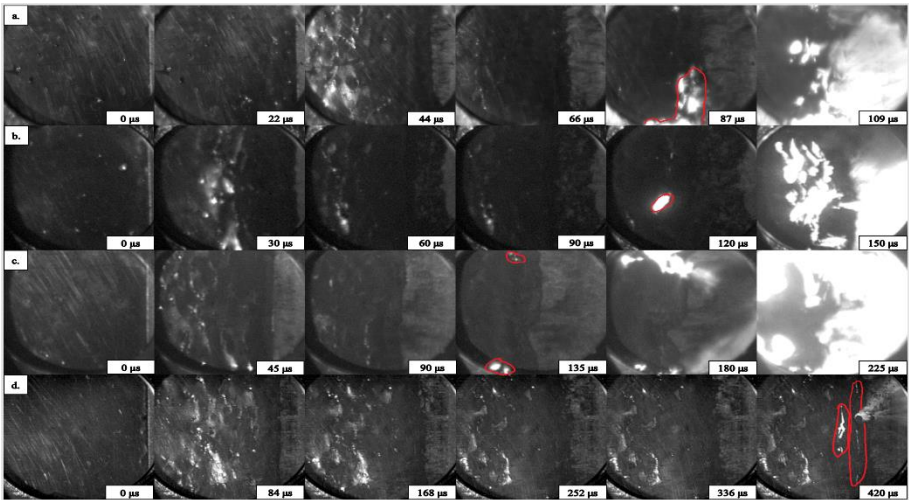
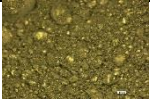
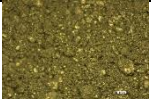
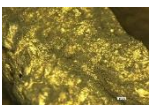



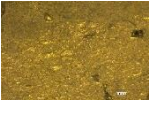
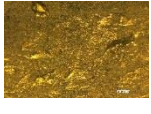


Figure 8: Still-frame images from Asay shear impact testing of 85% AIFA₅₀ with 15% large glass beads at (a) 124 m/s (b) 105 m/s (c) 69 m/s and (d) 35 m/s.

d. Characterization and modelling

With the results of the gas gun and Asay shear impact testing in mind, it now makes sense, perhaps, why the hand-molded samples reacted at lower velocities than the hot-pressed samples if one can assume there were likely more defects and inclusions in the hand-molded samples than in the hot-pressed samples. In an effort to quantify these differences optical microscopy, BET surface area and pore size measurements, and bomb calorimetry were executed on four samples: neat AIFA₅₀ powder, hot-pressed AIFA₅₀ post extrusion, ground AIFA₅₀ powder post extrusion, and hand-pressed AIFA₅₀ post extrusion. These samples are named AIFA-1, AIFA-4, AIFA-5, and AIFA-8, respectively.

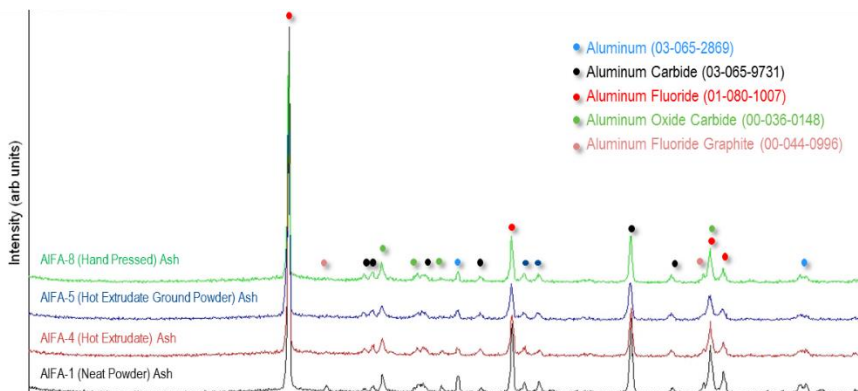
Table 4: Summary of optical microscopy, gas adsorption analysis and bomb calorimetry of various AIFA₅₀ samples.

Sample Name	Processing	Microscopy 100x	Microscopy 200x	Surface Area (m ² /g)	Pore Volume (cc/g)	Bomb Calorimetry (kJ/g)
AIFA-1	Neat Powder			5.034	0.012	5.56
AIFA-4	Hot Extrudate Hot-Pressed			0.930	0.000	5.37
AIFA-5	Hot Extrudate Ground Powder			1.119	0.002	5.47
AIFA-8	Hot Extrudate Hand-Molded			1.368	0.001	5.48

The hand-molded AIFA₅₀ (AIFA-8) had higher surface area and larger pore sizes than did the hot-pressed AIFA₅₀ (AIFA-4), indicating that the hand-molded liners contained more defects and pores which were likely responsible for the added sensitivity observed in ballistic testing for hand-molded specimens as compared to hot-pressed specimens.

The total energy released during bomb calorimetry was similar for all specimens with an average of 5.47 kJ/g, comparable to 2.175 kJ/g for TNT and 3.00 kJ/g for black powder. This indicates that the processing route does not necessarily affect the total exothermic output, but certainly may affect the sensitivity to ignition. X-ray diffraction was performed on the residues collected from the bomb calorimetry samples post-combustion, and the resulting diffraction patterns are shown in Figure 9. Interestingly, the analysis shows the presence of aluminium oxide carbide, not previously identified by Crouse et al. Residues from these pressurized bomb experiments show the presence of aluminium fluoride (AlF₃), aluminium carbide (Al₃C₄), aluminium oxide carbide (Al₄O₄C), and very small amounts of residual aluminium (Al) in all ash samples, and a small amount of aluminium fluoride

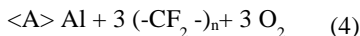
graphite in the ash of the neat powder only. No aluminium oxide (Al_2O_3) is present in any sample studied here, indicating that the chemical mechanism under pressurized bomb conditions is different than that reported by Crouse et al. for open-air combustion



experiments [1]. The preferred formation of $\text{Al}_4\text{O}_4\text{C}$ over Al_2O_3 under pressurized bomb conditions further strengthens the theory that the reaction mechanism and its kinetics are also, likely, a function of confinement. Interestingly, a very small $\text{Al}_4\text{O}_4\text{C}$ peak is observed in XRD of residues in literature [1], although the XRD peak is not identified nor is the existence of the phase discussed at all.

Figure 9: X-ray diffraction patterns of AIFA₅₀ residue collected post-reaction from bomb calorimetry.

In an effort to better understand the potential reaction mechanisms of AIFA nanocomposites, FactSage thermochemical modelling software was used to model the chemical reactions which may take place during combustion of AIFA₅₀, and to identify potential equilibrium reaction products for a variety of formulations and conditions. The use of FactSage software for modelling inorganic pyrotechnic reactions has been previously reported by Shaw et al. [12] for both adiabatic and non-adiabatic conditions. The AIFA combustion reaction was modelled by reacting Al with a pure fluorocarbon chain in the presence of oxygen as shown in Equation 4, wherein the moles of aluminium (<A>) can be varied to mimic the available chemistries of AIFA nanocomposites. For the AIFA₅₀ composite (50wt.% Al), <A> = 5.6 mol. The reaction assumes stoichiometric oxygen is available.



Crouse et al. reported that the product phases of the AIFA combustion reaction are AlF_3 , Al_2O_3 , Al_4C_3 , and residual Al, and that the mechanism proceeds preferentially from aluminium fluorination to oxidation to carburization with increasing aluminium content [1]. FactSage was used to understand how the amount of aluminium in the composite affects the predicted reaction products by varying the amount of Al in Equation 4 from 0 to 12 moles. The results of the predicted product phases are shown in Figure 10a. The thermochemical model confirms that the fluorination of aluminium occurs for all stoichiometric formulations where <A> > 0 mol. The model predicts some gas phase products for <A> < 6 mol. where total gases is > 99.99% CO_2 , with trace amounts of CO and COF_2 . The formation of Al_2O_3 occurs for <A> > 2 mol. in good agreement with the mechanism presented by Crouse et al. The thermodynamic model shows the formation of Al_2O_3 in variable amounts for all formulations with 2-8 mol of Al. The thermochemical software does, in fact, predict the

equilibrium formation of $\text{Al}_4\text{O}_4\text{C}$, but only when the Al content is greater than 6 moles, slightly more solids rich than the 5.6 moles theoretically available in the AlFA_{50} nanocomposites that were reacted in bomb calorimetry. Residual carbon in the form of graphite is predicted for Equation 4 at 298 K for $2 < \text{Al} > < 10$, although no graphite was identified in the ash analysed in this effort, or those analysed by Crouse et al. [1]. Finally, for $< \text{Al} > > 8$ mol. and for $< \text{Al} > > 10$ mol. the thermochemical model developed in FactSage predicts the formation of Al_4C_3 and residual Al, respectively. These results are, again, in good agreement with those presented by Crouse et al [1].

Figure 10b shows the predicted reaction enthalpy (ΔH_{rxn}) as a function of Al content, as well as the predicted adiabatic reaction temperature (T_{ad}) for the condition when $\Delta H = 0$. It can be seen that the enthalpy change approaches its maximum near 6 moles of Al, a formulation slightly richer in aluminium than the estimated 5.6 moles of Al available in the AlFA_{50} stoichiometry. The adiabatic reaction temperatures predicted for all chemistries is greater than 2298 K, with a slight maximum also occurring just below the AlFA_{50} stoichiometry at $< \text{Al} > = 5.2$ mol. Given the supreme adiabatic reaction temperatures that are possible, it is likely that any residual carbon that would be formed in equilibrium is likely oxidized to CO_2 during combustion when the reaction temperature is elevated.

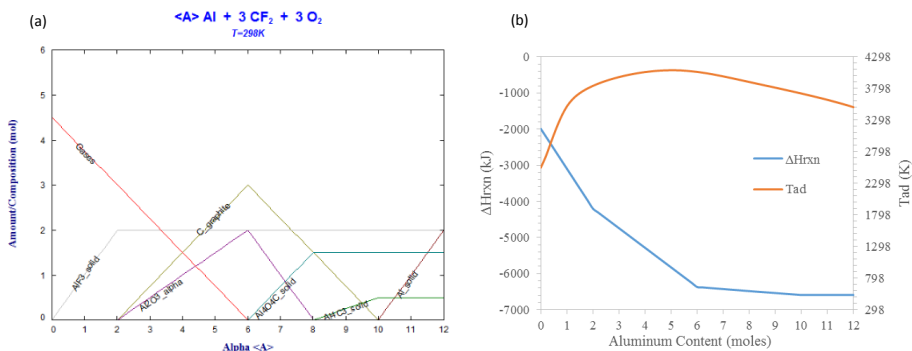


Figure 10: Results of thermochemical modelling using FactSage 7.1 for the combustion of AlFA_{50} showing (a) product phase formation as a function of moles of aluminum ($< \text{Al} >$) and (b) ΔH_{rxn} and adiabatic reaction temperature as a function of moles of aluminum.

The individual reactions that likely contribute to the AlFA combustion mechanism under various conditions are given in Table 5. These were each modelled by FactSage with the reactants at 298 K and 1 atm to determine the total enthalpy change (ΔH°), and the adiabatic reaction temperatures (T_{ad}) were calculated for $\Delta H = 0$; results are summarized in Table 5. Many of these reactions are extremely exothermic, each able to contribute to the large exothermic reaction observed when AlFA_{50} is ignited. While the actual reaction mechanism at play each time AlFA reacts is complicated and dependent on a number of factors including Al content and confinement, thermochemical models can aid in predicting product phases and reaction temperatures. It can be concluded that in addition to fluorination, oxidation, and carburization, the formation of $\text{Al}_4\text{O}_4\text{C}$ can also be one of the steps in the reaction mechanism.

Table 5: Thermodynamic properties of potential chemical reactions which may take place during AlFA₅₀ combustion as modelled with FactSage.

Reactions Modeled with FactSage	ΔH° (kJ)	T_{ad} (K)
$2 \text{ Al} + 3 \text{ CF}_2 \rightarrow \text{AlF}_3 + 3 \text{ C}$	-3018	3822
$2 \text{ Al} + 3/2 \text{ O}_2 \rightarrow \text{Al}_2\text{O}_3$	-2278	3992
$4 \text{ Al} + 3 \text{ C} \rightarrow \text{Al}_4\text{C}_3$	-220	1602
$4 \text{ Al} + \text{ C} + 2\text{O}_2 \rightarrow \text{Al}_4\text{O}_4\text{C}$	-2312	3724
$\text{C} + \text{O}_2 \rightarrow \text{CO}_2$	-404	3259

The types of thermochemical models used here to determine reaction pathways can be very useful in tuning the AlFA nanocomposite chemistry for specific applications, including bullet spotters, but the models are not perfect. These tools can help minimize the need to synthesize and test a large number of composites for, decreasing the cost of development and the potential for accidents in the laboratory. Unfortunately, however, the models are limited. In future work better models could be developed by creating a nanoaluminum reactant in the databases where the thermodynamic properties and surface potentials are captured for nAl separately from those for pure Al. The role kinetics plays in these reactions is also not predicted using equilibrium thermochemical models, and the fast kinetics of energetic reactions often forces the reactions to deviate from equilibrium. Finally, more robust models would have to be developed to start to incorporate sensitivity to ignition, as well as to determine what role inclusion materials might have on the reaction mechanisms and sensitivity.

IV. CONCLUSIONS

When the AlFA₅₀ reaction is initiated on impact it produces a fast, bright white, hot flash which can be detected easily by the naked eye and/or with infra-red optics. Ballistic testing revealed that the ignition threshold was near 80 m/s, and that it was beneficial to add tungsten shot behind the nanocomposite to help induce mechanical ignition upon impact. Hand-molded specimens were more prone to ignition than hot-pressed specimens at velocities less than 100 m/s. Gas gun testing confirmed a mechanical ignition mechanism, with ignition observed most often at a pinch point, when the AlFA₅₀ was confined between the target anvil and an incoming inert pusher. By systematically stepping down the launch velocity on the gas gun it was determined that the ignition threshold of AlFA₅₀ was between 70 and 75 m/s. An *extremely violent* reaction was observed near the ignition threshold (at 73 m/s), likely caused by a unique combination of mechanical and inertial confinement, with some added contribution from residual unreacted AlFA powder in the boom box. Multiple Asay shear experiments further confirmed the mechanically induced pinch ignition mechanism at play. It was found that ignition was possible at lower velocities (91 m/s) if a large pinch was induced by changing the impacting plunger from a rectangular to a parabolic geometry. When large glass beads (>1 mm) were used as an inclusion material ignition occurred at velocities as low as 39 m/s for a composite containing 85 vol.% AlFA₅₀ / 15 vol.% glass beads, demonstrating successful sensitization to a threshold velocity less than half of that observed in gas gun testing. The ignition delay time decreased parabolically with increasing impact velocity (sorry, where is the parabolic dependence? This was not mentioned or demonstrated above?). The total enthalpy of AlFA₅₀ reaction was determined to be 5.47 kJ/mol. The residue from bomb calorimetry was analysed and contained AlF₃, Al₄O₄C, and Al₄C₃, but no Al₂O₃.

Further characterization of hand-pressed and hot-pressed samples revealed more surface texture and included defects in the hand-pressed samples which likely contributed to the added sensitivity observed in ballistic testing. Finally, thermochemical modelling was used to explore equilibrium reaction products, enthalpy of reaction, and adiabatic reaction temperature all as a function of aluminium content. It was determined that the formation of Al_4O_4C should be considered an added step in the reaction mechanism of AIFA nanocomposites, although predicting the preferred pathway or reaction potential under various conditions and chemistries is complicated and a function of thermochemical equilibrium, reaction kinetics, and confinement.

V. REFERENCES

1. Crouse, Christopher A., Christian J. Pierce, and Jonathan E. Spowart. "Synthesis and reactivity of aluminized fluorinated acrylic (AIFA) nanocomposites." *Combustion and Flame* 159.10 (2012): 3199-3207.
2. Crouse, Christopher A., Jonathan E. Spowart. "Synthesis, reactivity, and mechanical properties of AIFA nanocomposites." TMS Annual Meeting, Orlando, FL. (12 March 2012).
3. Crouse, Christopher A., et al. "Particulate-based reactive nanocomposites and methods of making and using the same." U.S. Patent No. 9,120,710. 1 Sep. 2015.
4. Crouse C, Spowart J (2011) Dynamic behavior of reactive aluminium nanoparticle composite materials. In: Shock Compression of Condensed Matter 2011, Chicago, IL (Unpublished paper)
5. White, Bradley W., et al. "Impact initiation of reactive aluminized fluorinated acrylic nanocomposites." *Journal of Dynamic Behavior of Materials* 2.2 (2016): 259-271.
6. Perry, W. Lee, et al. "Interplay of explosive thermal reaction dynamics and structural confinement." *Journal of applied physics* 101.7 (2007): 074901.
7. Perry, W. Lee, et al. "Quantification of reaction violence and combustion enthalpy of plastic bonded explosive 9501 under strong confinement." *Journal of applied physics* 97.2 (2005): 023528.
8. Price, Donna, and J. F. Wehner. "The transition from burning to detonation in cast explosives." *Combustion and Flame* 9.1 (1965): 73-80.
9. Berghout, H. L., et al. "Combustion of damaged PBX 9501 explosive." *Thermochimica Acta* 384.1 (2002): 261-277.
10. Collignon, S.L., Burgess W.P., Wilson W.H., Gibson, K.D.. Proceedings for the Insensitive Munitions Technology Symposium, American Defence Preparedness Association, Williamsburg, VA (1992): 136.
11. Perry, W. Lee, et al. "Impact-induced friction ignition of an explosive: Infrared observations and modeling." *Journal of Applied Physics* 108.8 (2010): 084902.
12. Shaw, Anthony P., et al. "Thermodynamic Modeling of Pyrotechnic Smoke Compositions." *ACS Sustainable Chemistry & Engineering* 4.4 (2016): 2309-2315.